Novel multi-targeting anthra[2,3-b]thiophene-5,10-diones with guanidine-containing side chains: Interaction with telomeric G-quadruplex, inhibition of telomerase and topoisomerase…

ARTICLE *in* EUROPEAN JOURNAL OF MEDICINAL CHEMISTRY · AUGUST 2014

Impact Factor: 3.45 · DOI: 10.1016/j.ejmech.2014.08.030 · Source: PubMed

European Journal of Medicinal Chemistry 85 (2014) 605–614

Contents lists available at ScienceDirect

European Journal of Medicinal Chemistry

journal homepage: http://www.elsevier.com/locate/ejmech

Original article

Novel multi-targeting anthra[2,3-*b*]thiophene-5,10-diones with guanidine-containing side chains: Interaction with telomeric G-quadruplex, inhibition of telomerase and topoisomerase I and cytotoxic properties

Nikolay S. Ilyinsky [a, b, *], Anna K. Shchyolkina [a], Olga F. Borisova [a], Olga K. Mamaeva [a], Maria I. Zvereva [c], Dulat M. Azhibek [c, d], Mikhail A. Livshits [a, b], Vladimir A. Mitkevich [a], Jan Balzarini [e], Yuri B. Sinkevich [f], Yuri N. Luzikov [g], Lybov G. Dezhenkova [g], Ekaterina S. Kolotova [h, i], Alexander A. Shtil [h, i], Andrey E. Shchekotikhin [f, g, 1], Dmitry N. Kaluzhny [a, 1]

[a] *Engelhardt Institute of Molecular Biology, Russian Academy of Sciences, 32 Vavilov Street, Moscow 119991, Russia*
[b] *Department of Biological and Medical Physics, Moscow Institute of Physics and Technology, 9 Institutskiy Per., Dolgoprudny 141700, Russia*
[c] *Department of Chemistry, Lomonosov Moscow State University, GSP-1, 1-3 Leninskie Gory, Moscow 119991, Russia*
[d] *Skolkovo Institute of Science and Technology, 100 Novaya Street, Skolkovo 143025, Russia*
[e] *Rega Institute for Medical Research, KU Leuven, 3000 Leuven, Belgium*
[f] *Mendeleyev University of Chemical Technology, 9 Miusskaya Square, Moscow 125190, Russia*
[g] *Gause Institute of New Antibiotics, 11 B. Pirogovskaya Street, Moscow 119021, Russia*
[h] *Blokhin Cancer Center, 24 Kashirskoye Shosse, Moscow 115478, Russia*
[i] *Moscow Engineering and Physics Institute, 31 Kashirskoye Shosse, Moscow 115409, Russia*

ARTICLE INFO

Article history:
Received 20 March 2014
Received in revised form
5 August 2014
Accepted 7 August 2014
Available online 8 August 2014

Keywords:
Anthra[2,3-*b*]thiophene-5,10-dione
Telomeric DNA G-quadruplex
Telomerase
Topoisomerase I
Small molecular weight inhibitors
Cytotoxicity

ABSTRACT

Novel generations of antitumor anthraquinones are expected to be advantageous over the conventional chemotherapeutic agents. Previous structure–activity relationship studies demonstrated an importance of the positively charged side chains conjugated to anthra[2,3-*b*]thiophene-5,10-dione scaffolds. Exploring a role of individual side chain moieties in binding to the duplex and G-quadruplex DNA, modulation of telomerase and topoisomerase I activities, intracellular accumulation and cytostatic potency, we herein analyzed a series of reported and newly synthesized guanidine-containing derivatives of anthra[2,3-*b*]thiophene-5,10-dione. We found that the number of cationic side chains (namely, two) is critical for a tight interaction with human telomeric G-quadruplex (TelQ). Along with a larger drug–TelQ association constant, the telomerase attenuation by anthrathiophenediones with two basic groups in the side chains was more pronounced than by the analogs bearing one basic group. For mono-guanidinated compounds the substituent with the amino group in the side chain provided better TelQ affinity than the methylamine residue. The intracellular uptake of the mono-guanidino derivative with two side chains was >2-fold higher than the respective value for the bis(guanidino) derivative. This difference can explain a lower antiproliferative potency of bis(guanidine) containing compounds. Thus, the modifications of side chains of anthra[2,3-*b*]thiophene-5,10-dione differently modulated drug–target interactions and cellular effects. Nevertheless, the selected compound 11-(3-aminopropylamino)-4-(2-guanidinoethylamino)anthra[2,3-*b*]thiophene-5,10-dione **13** demonstrated a high affinity to TelQ and

Abbreviations: TelQ, human telomeric G-quadruplex in the presence of potassium ions; FRET, Förster resonance energy transfer; FAM, carboxyfluorescein; BHQ1, black hole quencher 1; G4-FID, G-quadruplex fluorescent intercalator displacement; TO, thiazole orange; ITC, isothermal titration calorimetry; RQ-TRAP, real-time quantitative telomeric repeat amplification protocol; PCR, polymerase chain reaction; IC_{50}, 50% growth inhibitory concentration; topo I, topoisomerase I.

* Corresponding author. Engelhardt Institute of Molecular Biology, Russian Academy of Sciences, 32 Vavilov Street, Moscow 119991, Russia.
E-mail address: ilinsky_nick@mail.ru (N.S. Ilyinsky).
[1] Authors share equal senior authorship.

http://dx.doi.org/10.1016/j.ejmech.2014.08.030

the ability to stabilize the quadruplex structure. These properties were paralleled by reasonable potency of **13** as a telomerase/topoisomerase I inhibitor and an antiproliferative agent. These results indicate that the structural elements of anthra[2,3-*b*]thiophene-5,10-dione derivatives can be balanced to yield a candidate for further preclinical study.

1. Introduction

The anthraquinone derivatives, an extensively investigated class of cytotoxic compounds, bind to a number of intracellular targets (reviewed in Ref. [1]) including various DNA conformations [2–4]. To explore the anticancer potential of anthraquinone derivatives, we have developed the synthesis of a series of anthra[2,3-*b*]thiophene-5,10-diones [5]. The selected compounds, in particular, 4,11-bis(2-(methylamino)ethylamino)anthra[2,3-*b*]thiophene-5,10-dione **1** (Fig. 1), demonstrated a high inhibitory potency against topoisomerase I (topo I) and promising cytotoxicity for mammalian tumor cell lines including multidrug-resistant counterparts. One may hypothesize that these therapeutically valuable activities are associated with the ability of anthra[2,3-*b*]thiophene-5,10-dione derivatives to bind to various DNA structures and interfere with DNA-operating enzymes. In line with this suggestion the introduction of basic groups with delocalized terminal cationic centers into the side chains of anthra[2,3*b*]thiophene-5,10-diones yielded the derivative **2** and its homologs capable of tight binding to DNA and RNA G-quadruplexes [6]. Moreover, the bis(guanidino) derivative **2** and its bis(amidino) analog **3** have been identified as multi-targeting agents with potent inhibition of topo I and telomerase [4,5]. Furthermore, **2** and its homologs accumulated in the cytoplasm and in the nuclei of several cancer cell lines; these compounds stabilized G-quadruplexes in the H-*Ras* oncogene promoter, an effect paralleled by a decreased H-*Ras* expression. Also, **2** and its homologs caused G1 arrest and strongly inhibited proliferation of T24 bladder cancer cells but not of non-malignant 293 or NIH 3T3 cell lines. Thus, bis(guanidine) **2** was identified as a promising prototype for development of agents that affect several targets critical for cancer cell viability. This polypharmacological approach is an emerging strategy for anticancer drug development [7–9].

The side chains of anthra[2,3-*b*]thiophene-5,10-diones with guanidine and amidine substituents have proved their importance. Nevertheless, the previously investigated compounds bearing these positively charged residues showed a poor cell permeability and low bioavailability [10,11]. Accordingly, the cytotoxicity of **2** (containing two guanidines) was less pronounced compared to the methylamino analog **1** [5]. Here, we investigated whether the number and the structure of terminal basic groups in the side chains influence the properties of mono-guanidinated anthrathiophenediones in cell-free systems and in cell culture. We provide evidence that, although chemical modifications of the side chains may yield the derivatives with variable properties, the structure can be optimized to produce the compound with promising antitumor characteristics.

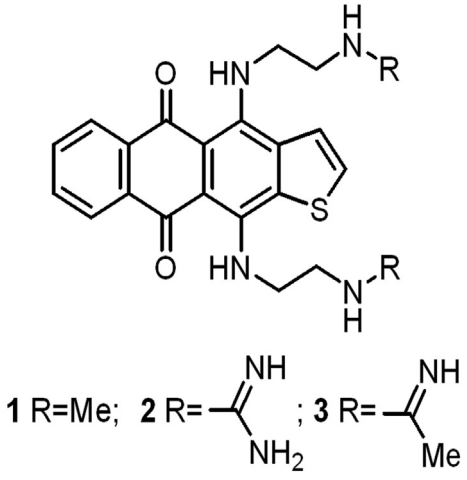

Fig. 1. Structure of anthrathiophenediones **1**–**3**.

2. Results and discussion

2.1. Chemistry

The synthesis of 4,11-diaminoanthrathiophenediones was accomplished by a nucleophilic substitution of alkoxy groups in the *peri*-position of 4,11-dibutoxyanthra[2,3-*b*]thiophene-5,10-dione **4** [12] with amines (Scheme 1). First, treatment of **4** with ammonia in methanol-THF yielded the core structure **5**. The methodology for synthesis of anthrathiophenediones bearing two different chains in positions 4 and 11 has been reported [6]. This approach is based on differential reactivity of alkoxy groups of **4** in the reaction of nucleophilic substitution. Treatment of **4** with 1,2-ethylenediamine at 30 °C for 3 h gave a mixture of mono-(aminoethyl)amino derivatives **6** and **7** that were separated by column chromatography (Scheme 1). The distal amino groups in isomers **6** and **7** were transformed into guanidine groups by treatment with pyrazole-1-carboxamidine, yielding the corresponding mono-guanidino derivatives **8** and **9**. The subsequent substitution of the butoxy group in **8** with ammonia, ethylenediamine, N-methylethylenediamine or 1,3-diaminopropane yielded anthra[2,3-*b*]thiophene-5,10-diones **10**–**13**, respectively, with guanidine groups in the side chains at the position 4 (Scheme 1). Likewise, anthra[2,3-*b*]thiophene-5,10-diones **14** and **15** bearing guanidine groups in the side chains at the position 11 were prepared from **9** (Scheme 1). All final monoguanidines **10**–**15** were purified by re-precipitation and gave good analytical and spectroscopic data in full accordance with their assigned structures.

2.2. Interaction with human telomeric G-quadruplex (TelQ) and duplex DNA

The telomeric DNA terminates in a single-stranded 3′ overhang which can form higher-order conformations termed G-quadruplexes. Stabilization of telomeric DNA as a G-quadruplex structure by selective small molecular weight compounds is aimed at down-regulation of telomerase activity and retardation of tumor cell growth [13]. Development of ligands with high affinity to G-quadruplex structures has proved to be a fruitful approach in anticancer drug design [14–16].

2.2.1. TelQ fold stabilization revealed by FRET (Förster resonance energy transfer) melting

Preferential binding of a ligand to G-quadruplex (compared to the binding to an unfolded DNA) means that the ligand is a G-

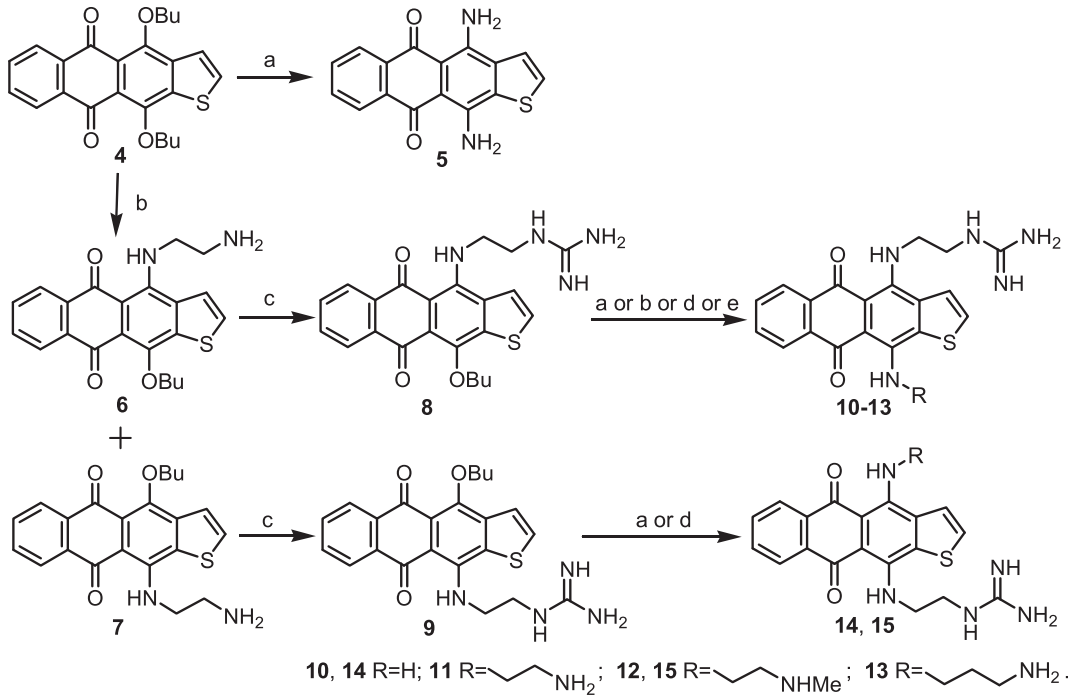

Scheme 1. Synthesis of anthra[2,3-*b*]thiophene-5,10-dione **5** and its (2-guanidinoethylamino)derivatives **10**–**15**. Reagents and conditions: (a) NH_3, THF-MeOH, 90 °C; (b) 1,2-ethylenediamine, THF, 30 °C, 3 h; (c) pyrazole-1-carboxamidine hydrochloride, EDIA, DMSO, 60 °C, 5 h; (d) N-methylethylenediamine, THF, 50 °C, 2 h; (e) 1,3-diaminopropane, THF, 50 °C, 2 h.

quadruplex stabilizer. It should be emphasized that some alteration of the structure accompanying the binding does not contradict the stabilization of the G-quadruplex fold. The stabilization is manifested by a rise of the DNA melting temperature in the presence of the ligand. The magnitude of the shift of melting temperature is determined by binding affinity. Therefore, the melting of G-quadruplex DNA in the presence of ligands has been used for a semi-quantitative testing of ligands' affinity to G-quadruplexes [17,18].

To our knowledge, this study is the first to apply FRET melting for quantitative assessment of ligand-target binding strength. The binding constant can be estimated by equation (1):

$$K_{\text{b FRET}} \simeq \frac{\exp\left(4\frac{\Delta T_m}{w}\right) - 1}{L}, \quad (1)$$

where ΔT_m is the melting temperature shift caused by ligand binding; w is the width of transition for free (unliganded) target molecule ($w = 23$ °C for TelQ22-DA under our experimental conditions, see Supplement); L is the total concentration of the ligand (1 μM). The detailed overview is presented in Supplement. This equation was used to assess the binding constants on the basis of experimental melting temperature shifts.

FRET melting assay allows for evaluating the binding constants only at the DNA melting temperature. However, these non-physiological values might be justified for comparison of ligands. The rating of compounds by $K_{\text{b FRET}}$ value can be obtained quickly and corresponds to their hierarchy at 36.6 °C.

FRET melting experiments were performed in buffer with K^+ ions. The nucleotide sequence TelQ22-DA labeled with the donor and the acceptor fluorescent molecules (FAM-5′-d(AGGGTTAGGGTTAGGGTTAGGG)-3′-BHQ1) mimics the single strand telomeric overhang. The FRET melting curves of TelQ22-DA with increasing concentrations of **2** and the first derivatives of these curves are shown in Fig. S1A, B (Supplement). We performed FRET melting of this oligonucleotide in complexes with new anthrathiophenediones **5**, **10**–**15** and reference analogs **1**–**3** using a 10-fold molar excess of ligands (1 μM of each compound, 0.1 μM (strand) of TelQ22-DA). The stabilization effects represented by ΔT_m, that is, the difference between melting temperatures with and without ligand ($T_m = 65$ °C for free TelQ22-DA), are summarized in Table 1. The binding constants evaluated by equation (1) are given in Table 1, column $K_{\text{b FRET}}$.

The circular dichroism and UV absorbance have shown that anthrathiophenediones can disrupt one G-quartet in a hybrid '3 + 1' conformation of TelQ formed in the presence of K^+ [4]. The stabilization showed by FRET seems to contradict this finding. We suppose that FRET melting reveals the stabilization of the fold of the sugar-phosphate backbone without one G-tetrad rather than the initial TelQ structure. This DNA fold may inhibit telomerase activity similarly to the G-quadruplex because both DNA conformations provide steric hindrances for complementary binding of the RNA template of the catalytic telomerase subunit TERT (telomerase reverse transcriptase).

2.2.2. Competitive FRET melting

Competitive FRET melting was performed for the best stabilizers **2** and **13** (Fig. S2, Supplement). Various concentrations of double stranded (ds) DNA (ds26 (5′-d(CAATCGGATCGAATTCGATCCGATTG)-3′)) were added to the mixture of TelQ and anthrathiophenedione. The presence of ds26 competitor diminishes the ligand-induced TelQ stabilization. The dsDNA markedly pulled the ligand out of TelQ. A 110-fold molar excess of ds26 over TelQ22-DA (in base pairs over base quartets) abrogated the stabilization effect of **2**; compound **13** was slightly more preferential to TelQ. Thus, the compounds had no substantial selectivity for TelQ.

Table 1
Thermal stabilization of TelQ, binding affinity and antiproliferative activity of novel anthrathiophenediones **5**, **10**–**15** and reference compounds **1**–**3**.

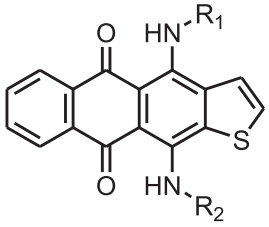

#	R_1	R_2	ΔT_m[a], °C	$K_{b\ FRET}$[b] (10^6, M^{-1}) at 65 °C	$K_{b\ FID}$[c] (10^6, M^{-1}) at 25 °C	$K_{b\ ITC}$[d] (10^6, M^{-1}) at 25 °C	IC_{50}[e], μM	
							(L1210)	(CEM)
5	H	H	0.1 ± 0.9	~0.01	1.3 ± 0.3	nd[f]	>250	>250
10	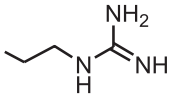	H	1 ± 1	0.2 ± 0.2	1.6 ± 0.2	0.6 ± 0.1	19 ± 6	16 ± 3
14	H	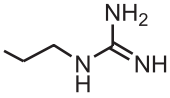	1 ± 1	0.1 ± 0.2	2.1 ± 0.7	0.5 ± 0.1	22 ± 5	21 ± 2
12	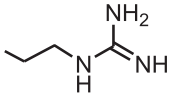	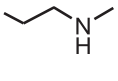	5.4 ± 0.8	1.6 ± 0.4	5.5 ± 0.8	4.9 ± 0.9	23 ± 5	6 ± 2
15		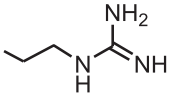	5.1 ± 0.6	1.5 ± 0.3	4 ± 1	2.5 ± 0.4	16 ± 7	11 ± 3
11	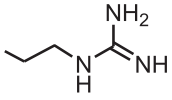	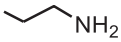	5 ± 2	1.5 ± 0.7	12 ± 2	11 ± 2	16 ± 5	7 ± 1
13	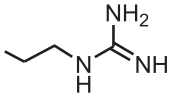	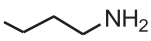	10 ± 3	5 ± 2	9 ± 1	3.7 ± 0.7	10 ± 3	10 ± 2
1			4.3 ± 1.4	1.1 ± 0.5	11 ± 2	1.6 ± 0.3	0.9 ± 0.2	0.4 ± 0.1
2	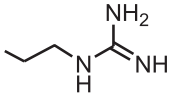	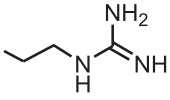	12 ± 2	7 ± 3	8 ± 2	nd	20 ± 3	11 ± 2
3	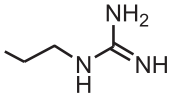	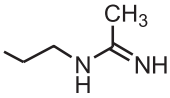	7 ± 1	2.4 ± 0.8	8 ± 2	1.1 ± 0.2	36 ± 4	39 ± 2

[a] ΔT_m, mean ± standard deviation (S.D.) of three independent experiments.
[b] $K_{b\ FRET}$, mean ± S.D. of 3 experiments, calculated from equation (1).
[c] $K_{b\ FID}$, mean ± S.D. of 3 experiments, assessed by equation (2) for each ligand concentration during titration and averaged in every experiment.
[d] $K_{b\ ITC}$, mean ± S.D. of 3 experiments.
[e] IC_{50} (50% growth inhibitory concentration), mean ± S.D. of 3 experiments (see Material and Methods).
[f] not determined.

2.2.3. Affinity of anthrathiophenediones to TelQ determined by G4-FID (G-quadruplex fluorescent intercalator displacement) assay

The affinity of compounds to TelQ24 (5′-d(TTAGGG)$_4$)-3′) was independently evaluated using G4-FID assay. The mixture of TelQ and thiazole orange (TO) fluorophore was titrated with ligands, and TO displacement was monitored by the decrease of TO fluorescence (Fig. S3, Supplement; experimental conditions are in Materials and Methods). The binding constants were assessed by the equation (2) (see Supplement for details):

$$K_{b\ FID} = \left(\frac{I(0)}{I(L)} - 1\right) \cdot \frac{1 + K_F F}{L}, \quad (2)$$

where $K_{b\ FID}$ and K_F are the association constants of the ligand and TO with TelQ, L and F are the concentrations of the ligand and TO ($F = 1$ μM); I(0) and I(L) are TO fluorescence intensities without ligand and at the ligand concentration L. The association constant of TO–TelQ binding in 100 mM KCl is $K_F = 2 \times 10^6$ M^{-1} [19]. The

binding constants of anthrathiophenediones to TelQ evaluated by equation (2) are given in Table 1, column $K_{b\ FID}$.

2.2.4. Ligand–TelQ affinity determined by ITC (isotermal titration calorimetry)

Interactions between TelQ22 (5′-d(AGGG(TTAGGG)$_3$)-3′) and anthrathiophenediones were also studied by ITC at 25 °C. Values of $K_{b\ ITC}$ are shown in Table 1; thermodynamic parameters of binding are presented in Table S1, Supplement. Parameters for **2** and **5** were not defined because of poor water solubility and aggregation of molecules at close-to-physiological temperature, pH and ionic strength of the buffer. Table 1 shows that the values of binding constants determined by ITC and G4-FID were close. The rating of compounds based on $K_{b\ FRET}$ is identical to that obtained with G4-FID and ITC.

Novel anthrathiophenediones fell into three categories based on TelQ binding constants (Table 1). First, compounds **5**, **10**, **14** without terminal basic group or with one such group weakly bind to TelQ ($\Delta T_m \leq 1$ °C, $K_b \leq 6 \times 10^5$ M^{-1} (at 25 °C)). Second, **12** and **15**, with two basic substituents (methylamine and guanidine), showed a moderate affinity ($\Delta T_m \sim 5$ °C, $K_b \leq 5 \times 10^6$ M^{-1}). Third, the di-substituted mono-guanidino derivatives **11**, **13** were reasonably good TelQ binders (5 °C $\leq \Delta T_m \leq$ 10 °C, $K_b \sim 10^7$ M^{-1}).

2.3. Anthrathiophenediones inhibit DNA enzymes

2.3.1. Effects on telomerase-mediated DNA elongation

We next tested the ability of anthrathiophenedione derivatives to modulate the activity of telomerase *in vitro*. We used the Real-time Quantitative Telomeric Repeat Amplification Protocol (RQ-TRAP) assay [20–22] to determine the influence of compounds on elongation of the telomerase substrate 5′-d(AATCCGTCGAGCAGAGTT)-3′ (TS) by telomerase partially purified from HEK293T cell lysates.

Given that the procedure presumes the presence of the compound in the telomerase reaction mixture (i.e., elongation of TS oligonucleotide) and, after dilution, in the PCR mixture, it is important to compare the concentrations of compounds that attenuated each of these reactions. The concentration of **5** that attenuated PCR by 50% was 33 μM (Fig. 2A and Table 2). Fig. 2B (○) demonstrates that the amount of **5** left after the telomerase reaction mixture was diluted 1:1180 (see Material and Methods) had no effect on PCR. Therefore, the decreased yield of the PCR products (●) after telomerase elongation cannot be attributed to inhibition of the PCR step but is due to telomerase attenuation. Values of $^{tel}IC_{50}$ and $^{PCR}IC_{50}$ for other tested anthrathiophenedione derivatives are given in Table 2. Submicromolar and micromolar values of $^{PCR}IC_{50}$ are in line with results reported for other compounds [23].

Table 2
Effects of anthrathiophenedione derivatives on telomerase-mediated DNA extension and on PCR.

#	$^{tel}IC_{50}$[a], μM	$^{PCR}IC_{50}$[b], μM
5	10 ± 2	33 ± 23
10	2.0 ± 0.7	0.9 ± 0.3
14	3.0 ± 0.9	0.5 ± 0.3
12	0.6 ± 0.2	0.30 ± 0.07
15	1.1 ± 0.5	0.05 ± 0.03
11	0.8 ± 0.2	0.10 ± 0.06
13	0.7 ± 0.2	0.07 ± 0.05
1	0.7 ± 0.2	0.5 ± 0.1
2	0.7 ± 0.3	0.08 ± 0.01
3	0.47 ± 0.14	0.30 ± 0.07

IC_{50}, mean ± S.D. of 3 independent experiments.
[a] $^{tel}IC_{50}$, 50% telomerase inhibitory concentration.
[b] $^{PCR}IC_{50}$, 50% PCR inhibitory concentration.

Data in Table 2 showed that the compounds inhibited telomerase activity at micromolar concentrations. Similar telomerase inhibitory potencies have been reported for other ligands that stabilize TelQ folds. For example, water soluble perylene diimides inhibited telomerase at 0.5–5 μM depending on the number and the type of the side chains [24]. Furthermore, the anti-telomerase potency of **5**, **10**, **14** with no or one side chain was inferior to the respective values for compounds with two side chains. A lower affinity of **5**, **10**, **14** to TelQ ($K_b \sim 10^5$ M^{-1} *vs* $> 10^6$ M^{-1} for other compounds, Table 1) correlates with this observation. All other compounds demonstrated $^{tel}IC_{50} \sim 1$ μM, so differences in chemical structure had no effect on telomerase inhibition. Compounds **2**, **11** and **13** showed similar IC_{50} values against telomerase, consistent with their ranking in TelQ stabilization (Table 1). Thus, the substitution of one guanidine by an amine did not change the binding to TelQ, nor did this modification alter telomerase activity.

2.3.2. Topo I inhibition

Novel derivatives of 4,11-diaminoanthra[2,3-*b*]thiophene-5,10-dione effectively bind to TelQ and duplex DNA, and inhibit

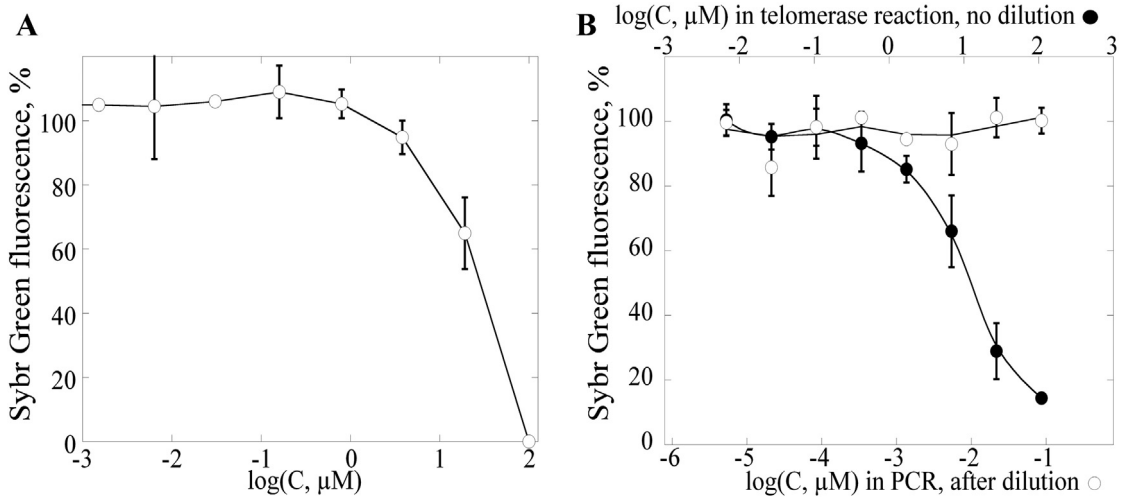

Fig. 2. A. Inhibition of PCR by compound **5**. B. Inhibition of telomerase (●) and PCR after dilution (○) by **5**. Compound's concentrations in the telomerase elongation reaction are shown on the top axis. The amounts of **5** in PCR mixture after 1:1180 dilution of the telomerase reaction mixture are plotted on the bottom axis. Values are mean ± S.D. of 3 experiments. Results for other anthrathiophenedione derivatives are presented in Figs. S4, S5, Supplement.

telomerase-mediated DNA elongation. Previously we have reported that compounds **1** and **2** can block topo I mediated DNA relaxation [5]. Therefore, we tested new compounds for the ability to modulate topo I activity. Fig. 3 shows the topoisomers of pBR322 plasmid generated by topo I in the absence or presence of **1**, **2**, **11**, **13**–**15**. Results with other compounds are shown in Fig. S6, Supplement.

The topo I mediated plasmid relaxation was significantly attenuated by 1 μM of **1**–**3** and **11**–**14**. Compounds **5**, **10** with zero or just one side chain were less potent (Fig. S6), which is in line with their substantially smaller affinity to DNA (compared with compounds with two side chains, Table 1). Thus, the number of side chains is important for topo I inhibition. The compounds with different terminal side chain residues showed similar topo I modulation potencies.

2.4. Activity in cell culture

The experiments analyzed above demonstrated that bis(guanidine) **2** and its mono-guanidino analog **13** were the most potent DNA binders/TelQ stabilizers (K_b ~ 5 × 10^6 M^{-1} (at 25 °C), $\Delta T_m \approx 10$ °C, Table 1). Furthermore, **13** retained the ability of **2** to attenuate telomerase and topo I in cell-free systems (Table 2 and Fig. 3). One may hypothesize that modification that yielded **13** represents the preferred way to optimize anthrathiophenediones as anticancer agents. We compared two key characteristics, that is, intracellular accumulation and cytotoxicity, of anthra[2,3-*b*]thiophene-5,10-dione **13** with one guanidine residue in the side chains and the initial compound **2**. Compound **1** bearing no guanidines was tested for comparison.

2.4.1. Intracellular accumulation of anthrathiophenedione derivatives

To check intracellular uptake, the L1210 cells were loaded with **1**, **2** or **13** (1 μM each) followed by flow cytometry (Fig. 4). The fluorescence intensities were obtained from 660/20 channel on Red HeNe trigon (excitation wavelength 633 nm) and were normalized to the intensity of autofluorescence of free compounds in DMSO (see Materials and Methods).

Compounds **1**, **2** and **13** entered the cells within the initial 15 min of incubation. Accumulation of bis(guanidine) **2** remained nearly constant for 3 h. In contrast, the intensities of intracellular fluorescence for **1** and **13** varied. Maximum fluorescence was observed after 60 min, the subsequent decrease can be attributed to the drug efflux. Remarkably, intracellular accumulation of monoguanidine **13**, although smaller than that of **1**, was significantly greater than the uptake of **2** over the entire time of incubation.

2.4.2. Antiproliferative activity of anthrathiophenediones

This activity was evaluated against murine leukemia L1210 and human T-lymphocyte CEM tumor cell lines (Table 1, the rightmost columns). Only **1** containing methylaminoethyl groups in the side chains, the compound that showed the most pronounced intracellular accumulation (Fig. 4), was markedly toxic (IC_{50} < 1 μM for both cell lines, Table 1). Compounds **10**–**12**, **14** and **15** with one or two side chains, bearing only one guanidine group, as well as bis(guanidine) **2** inhibited tumor cell proliferation at micromolar concentrations (Table 1). In line with its better intracellular accumulation, **13** was somewhat more potent than **2** in inhibiting proliferation of L1210 cells (IC_{50} 10 ± 3 μM and 20 ± 3 μM, respectively; Table 1). These results indicated that structural modifications of side chains may result in diverse effects on individual, therapeutically relevant properties of anthrathiophenediones.

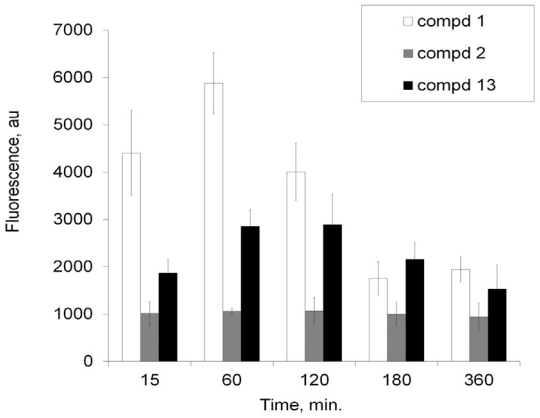

Fig. 4. Intracellular accumulation of **1**, **2** and **13**. The L1210 cells were loaded with compounds (1 μM each) for indicated time intervals at 37 °C, 5% CO_2 and washed with cold saline and immediately analyzed by flow cytometry. Ten thousand events were collected per each sample. Values (arbitrary units, a.u.; mean ± S.D. of 3 independent experiments) represent fluorescence channels of histograms' peaks normalized to autofluorescence of solutions containing 1 μM of **1**, **2** or **13**.

3. Conclusion

The analysis of the expanded series of anthrathiophenedione derivatives (previously reported **1**–**3** and newly synthesized **5**, **10**–**15**) provides important structure–activity relationship considerations. Introduction of two basic groups with delocalized terminal cationic centers into the side chains of **1**, such as acetamidines (**3**) and guanidines (**2**) enhanced the TelQ stabilizing potency (Table 1). Due to properties of guanidine and amidine residues (the former has a higher basicity [25,26] and better H-bond donating ability), the TelQ binding constant of bis(guanidine) **2** is greater than that of bis(amidine) **3**.

The core structure **5** that lacks side chains, as well as compounds **10** and **14** with one single side chain, evoked little-to-null effect on TelQ thermostability. Introduction into the anthrathiophenedione scaffold of the second side chain with methylamino or amino groups (compounds **11**–**13**, **15**) increased the affinity to TelQ compared to **10** or **14**. These results indicated that the number of cationic side chains is a critical factor for tight binding to TelQ; the interaction of anthrathiophenedione's aromatic core with TelQ is

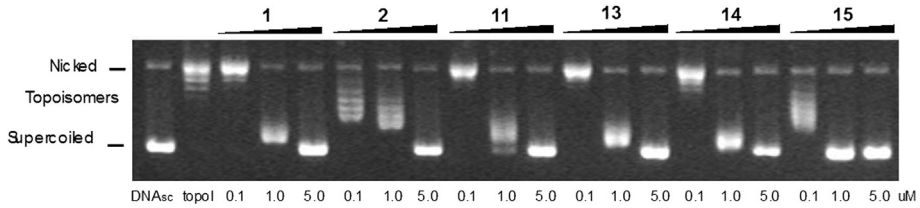

Fig. 3. Influence of anthra[2,3-*b*]thiophene-5,10-diones **1**, **2**, **11**, **13**–**15** on topo I activity. Lanes: DNAsc, supercoiled pBR322 plasmid; topo I, supercoiled pBR322 plasmid incubated with topo I alone. Other lanes: DNA topoisomers (positions are shown to the left) after topo I-mediated relaxation in the presence of indicated concentrations of tested compounds.

insufficient for a strong complex formation. The role of side chain substituents is important. The methylamino residue provides a lower TelQ affinity of **12**, **15** in comparison with that for **11** and **13** with amino substituents. Replacement of one methylamine with guanidine improves the affinity to TelQ since the binding constants of mono-guanidino derivatives **12**, **15** are higher than that of **1** bearing two methylamino groups. On the other hand, substitution of one guanidine group in **2** for amine in **13** slightly altered the stabilization effect. Therefore, two guanidines in the side chains are not mandatory for binding of anthrathiophenediones to TelQ. Isomers with altered position of side chains stabilized TelQ to a similar extent (compare **10** and **14**, **12** and **15**), so the orientation of the heterocyclic moiety did not affect binding to TelQ.

Structural optimization of anthrathiophenediones presumes a proper balance between the parameters of drug–target interaction *in vitro* and activities in cell culture. Importantly, cell-permeable **13** bearing one single guanidine residue showed a high TelQ binding constant and stabilization potency. The antiproliferative activity of this compound was lower than that of **1** (Table 1). However, a moderate cytotoxicity is likely to be desirable if the telomerase inhibitory potency is retained (discussed in Ref. [27]). The net antiproliferative effect of quadruplex ligands is expected to be achieved not as much by a short-term (up to 72 h) cytotoxicity but rather via a delayed growth retardation associated with telomerase inhibition. One may hypothesize that such a 'shift' of antitumor potencies would be advantageous for limiting compound's general toxicity *in vivo*. A detailed analysis of **13** against a panel of tumor and non-malignant cell lines is under way; these experiments as well as *in vivo* testing will determine whether this anthrathiophenedione derivative can be considered as a preferred drug candidate.

4. Materials and methods

4.1. General

The NMR spectra of all newly synthesized compounds were obtained with a 400 MHz (^{1}H NMR) and 100 MHz (^{13}C NMR) Varian VXR-400 instrument (Palo Alto, USA). Chemical shifts were measured in DMSO-d_6 using tetramethylsilane as an internal standard. Analytical TLC was performed on silica gel F254 plates, and column chromatography on Silica Gel 60 (Merck, Darmstadt, Germany). Melting points were determined on a Buchi SMP-20 apparatus (Flawil, Switzerland) and are uncorrected. High resolution mass spectra were recorded by electron spray ionization on a Bruker Daltonics micrOTOF-QII instrument (Bremen, Germany). UV spectra were recorded on Hitachi-U2000 spectrophotometer (Tokyo, Japan). HPLC was performed using Shimadzu Class-VP V6.12SP1 system (Kromasil-100-5 μm C-18 column, 4.6 mm × 250 mm, Kyoto, Japan). Eluents: A, H_3PO_4 (0.01 M); B, MeCN. All solutions were evaporated at a reduced pressure on a Buchi-R200 rotary evaporator (Flawil, Switzerland) at $t^\circ < 50$ °C. All products were vacuum dried at room temperature. All solvents, chemicals and reagents were obtained from Sigma–Aldrich, St. Louis, USA (unless specified otherwise) and used without purification. Compounds **4**, **6**, **7** were prepared as described [5,12]. The purity of new compounds **5**, **8**–**15** was >95% as determined by HPLC analysis. The purity of **5** was also confirmed by elemental analysis. Anthra[2,3-*b*]thiophene-5,10-diones **1**–**3**, **10**–**15** were tested as corresponding hydrochlorides.

The oligonucleotides TelQ22-DA (FAM-5′-d(AGGGTTAGGGTTAGGGTTAGGG)-3′-BHQ1; FAM, carboxyfluorescein; BHQ1, black hole quencher 1), TelQ24 (d(TTAGGG)$_4$), TelQ22 (5′-d(AGGGTTAGGGTTAGGGTTAGGG) and ds26 (5′-d(CAATCGGATCGAATTCGATCCGATTG)-3′) were synthesized and purified by Syntol (Moscow, Russia). All single stranded oligonucleotides were diluted in respective buffers and pre-annealed (95 °C for 10 min followed by cooling on ice for 10 min) prior to the experiments.

4.2. Synthesis of anthra[2,3-b]thiophene-5,10-diones **5**, **8**–**15**

4.2.1. 4,11-Diaminoanthra[2,3-b]thiophene-5,10-dione (**5**)

A stirred mixture of anthrathiophenedione **4** [12] (80 mg, 0.2 mmol), anhydrous solution of ammonia in methanol (10%, 5 mL) and 1,4-dioxane (5 mL) in a sealed tube was heated at 90–95 °C for 6–8 h. During this time the yellow color of the reaction mixture changed to violet, and after complete conversion of **4** (as determined by TLC) the solution was cooled and quenched with water. The product was precipitated, collected by filtration, dried and crystallized from chlorobenzene–DMF mixture (2:1) to yield **5** (44 mg, 76%) as dark blue crystals, mp 278–280 °C. HPLC (LW = 262 nm, gradient B 40 → 60% (20 min)) t_R = 19.21 min, purity 95.7%. ^{1}H NMR (400 MHz, DMSO-d_6) δ 8.92 (br s, 4H, NH_2), 8.26 (m, 2H, 6-H, 9-H), 8.09 (s, 2H, 2-H, 3-H), 7.78 (m, 2H, 7-H, 8-H); ^{13}C NMR (100 MHz, DMSO-d_6) δ 181.45 (C=O), 181.02 (C=O), 144.18 (C), 142.88 (C), 136.03 (C), 135.50 (C), 134.57 (C), 134.30 (C), 104.91 (C), 104.66 (C),132.34 (CH), 132.24 (CH), 131.30 (CH), 125.83 (2CH), 124.17 (CH); UV (ethanol) λ_{max} (log ε) 262 (4.5), 305 (3.6), 498 sh (3.7), 531 (4.0), 569 (4.1) nm. HRMS (ESI) calculated for $C_{16}H_{11}N_2O_2S$ $[M+H]^+$ 295.0536, found 295.0529. Analysis calculated for $C_{16}H_{10}N_2O_2S$: C 65.29, H 3.42, N 9.52. Found: C 65.02, H 3.59, N 9.63.

4.2.2. 11-Butoxy-4-(2-guanidinoethylamino)anthra[2,3-b]thiophene-5,10-dione hydrochloride (**8**)

To a stirring solution of **6** [5] (390 mg, 0.1 mmol) in acetonitrile (10 mL) ethyldiisopropylamine (0.5 mL, 0.35 mmol) and pyrazole-1-carboxamidine hydrochloride (50 mg, 0.35 mmol) were added. The mixture was stirred for 5 h at 60 °C and then cooled. The precipitated product was collected by filtration. The dark violet solid was re-precipitated from hot water with acetone-ether mixture (2:1), washed with acetone and, after drying, yielded hydrochloride **8** (339 mg, 72%). HPLC (LW = 263 nm, gradient B 30 → 70% (30 min)) t_R = 19.45 min, purity 97.7%. ^{1}H NMR (400 MHz, DMSO-d_6) δ 11.57 (t, 1H, J = 5.0 Hz, NH), 8.15 (m, 2H, 6-H, 9-H), 8.02 (s, 2H, 2-H, 3-H), 7.94 (br s, 1H, NH), 7.82 (m, 2H, 7-H, 8-H), 7.25 (br s, 4H, $2NH_2$), 4.04 (t, 2H, J = 6.4 Hz, OCH_2), 3.95 (m, 2H, $HNCH_2$), 3.56 (m, 2H, CH_2NH), 1.81 (m, 2H, $OCH_2CH_2CH_2$), 1.54 (m, 2H, CH_2CH_3), 0.98 (t, 3H, J = 7.4 Hz, CH_3). ^{13}C NMR (100 MHz, DMSO-d_6) δ 182.79 (C=O), 182.02 (C=O), 157.21 (C), 148.04 (C), 146.83 (C), 145.13 (C), 134.49 (C), 133.37 (C), 131.95 (C), 118.52, (C), 108.46 (C), 133.77 (CH), 133.08 (CH), 130.41 (CH), 126.85 (CH), 126.13 (CH), 125.96 (CH), 73.29 (CH_2), 45.42 (CH_2), 41.10 (CH_2), 32.02 (CH_2), 18.79 (CH_2), 13.85 (CH_3). UV (ethanol) λ_{max} (log ε) 263 (4.5), 310 (3.6), 519 (3.8), 558 sh (3.7) nm. HRMS (ESI) calculated for $C_{23}H_{25}N_4O_3S$ $[M+H]^+$ 437.1642, found 437.1650.

4.2.3. 4-Butoxy-11-(2-guanidinoethylamino)anthra[2,3-b]thiophene-5,10-dione hydrochloride (**9**)

This compound was prepared from anthrathiophenedione **7** [5] as described for **8**. Dark violet powder, yield 70%. HPLC (LW = 262 nm, gradient B 30 → 70% (30 min)) t_R = 18.60 min, purity 96.4%. ^{1}H NMR (400 MHz, DMSO-d_6) δ 11.51 (t, 1H, J = 5.4 Hz, NH), 8.22 (d, 2H, J = 5.5 Hz, 2-H), 8.14 (m, 2H, 6-H, 9-H), 7.99 (br s, 1H, NH), 7.79 (m, 2H, 7-H, 8-H), 7.64 (d, 2H, J = 5.5 Hz, 3-H), 7.21 (br s, 4H, $2NH_2$), 4.05 (m, 2H, $HNCH_2$), 3.98 (t, 2H, J = 6.5 Hz, OCH_2), 3.55 (m, 2H, CH_2NH), 1.81 (m, 2H, $OCH_2CH_2CH_2$), 1.50 (m, 2H, CH_2CH_3), 0.97 (t, 3H, J = 7.4 Hz, CH_3). UV (ethanol) λ_{max} (log ε) 262 (4.5), 322 (3.6), 511 (3.8), 553 sh (3.7) nm. HRMS (ESI) calculated for $C_{23}H_{25}N_4O_3S$ $[M+H]^+$ 437.1642, found 437.1651.

4.2.4. 11-Amino-4-(2-guanidinoethylamino)anthra[2,3-b] thiophene-5,10-dione hydrochloride (**10**)

A stirred mixture of **8** (90 mg, 0.2 mmol), anhydrous solution of ammonia in methanol (10%, 5 mL) and 1,4-dioxane (5 mL) in a sealed tube was heated at 90–95 °C for 8–10 h. After complete conversion of **8** (as determined by TLC) the mixture was evaporated. The residual compound was dissolved in hot water (2–3 mL) and acidified with two drops of hydrochloric acid. The solution was filtered, the product was precipitated with the mixture of acetone-ether (2:1), collected by filtration and dried. The yield of hydrochloride **10** was 56 mg (71%), mp 255–257 °C. HPLC (LW = 264 nm, gradient B 30 → 70% (30 min)) t_R = 11.42 min, purity 96.7%. ^{1}H NMR (400 MHz, DMSO-d_6) δ 11.24 (t, 1H, J = 5.1 Hz, NH), 8.95 (br s, 2H, NH_2), 8.29 (m, 3H, 6-H, 9-H, NH), 8.12 (d, 1H, J = 5.6 Hz, 2-H), 8.01 (d, 1H, J = 5.6 Hz, 3-H), 7.79 (m, 2H, 7-H, 8-H), 7.20 (br s, 4H, $2NH_2$), 3.95 (m, 2H, $HNCH_2$), 3.53 (m, 2H, CH_2NH). UV (ethanol) λ_{max} (log ε) 264 (4.5), 310 (3.6), 544 (4.0), 585 (4.2) nm. HRMS (ESI) calculated for $C_{19}H_{18}N_5O_2S$ $[M+H]^+$ 380.1176, found 380.1165.

4.2.5. 11-(2-Aminoethylamino)-4-(2-guanidinoethylamino)anthra [2,3-b]thiophene-5,10-dione dihydrochloride (**11**)

A mixture of **8** (90 mg, 0.2 mmol), 1,2-ethylenediamine (1 mL) and 1,4-dioxane (2 mL) was heated at 50 °C for 3 h. After complete conversion of **8** (as determined by TLC) the mixture was evaporated. The residue was purified by column chromatography with chloroform–methanol–concd NH_4OH (5:1:0 → 3:2:1) as eluting solvent. The residual compound was dissolved in hot water (2–3 mL), acidified with two drops of hydrochloric acid, filtered, then precipitated with acetone-ether mixture (1:1), collected by filtration and dried. The yield of dihydrochloride **11** was 59 mg (68%) as a dark blue solid, mp 208–210 °C (dec). HPLC (LW = 266 nm, gradient B 10 → 70% (30 min)) t_R = 11.06 min, purity 99.2%. ^{1}H NMR (400 MHz, DMSO-d_6) δ 12.00 (br s, 2H, 2NH), 8.27 (m, 4H, 2-H, 6-H, 9-H, NH), 8.04 (d, 1H, J = 5.5 Hz, 3-H), 7.82 (m, 2H, 7-H, 8-H), 7.25 (br s, 4H, $2NH_2$), 4.14 (m, 2H, $HNCH_2$), 3.91 (m, 2H, $HNCH_2$), 3.53 (m, 2H, $HNCH_2CH_2$), 3.22 (m, 2H, $HNCH_2CH_2$). HRMS (ESI) calculated for $C_{21}H_{23}N_6O_2S$ $[M+H]^+$ 423.1598, found 423.1597.

4.2.6. 4-(2-Guanidinoethylamino)-11-(2-(methylamino) ethylamino)anthra[2,3-b]thiophene-5,10-dione dihydrochloride (**12**)

This compound was prepared from **8** and N-methylethylenediamine as described for **11**. A dark blue powder, yield 72%, mp 199–201 °C. HPLC (LW = 266 nm, gradient B 10 → 60% (25 min)) t_R = 12.78 min, purity 97.2%. ^{1}H NMR (400 MHz, DMSO-d_6) δ 11.97 (br s, 2H, 2NH), 9.33 (br s, 2H, 2NH), 8.22 (m, 3H, 2-H, 6-H, 9-H), 8.02 (d, 1H, J = 5.5 Hz, 3-H), 7.94 (t, 1H, J = 5.6 Hz, NH), 7.78 (m, 2H, 7-H, 8-H), 7.30 (br s, 4H, $2NH_2$), 4.21 (m, 2H, $HNCH_2$), 3.90 (m, 2H, $HNCH_2$), 3.52 (m, 2H, $HNCH_2CH_2$), 3.31 (m, 2H, $HNCH_2CH_2$), 2.62 (t, 3H, J = 5.3 Hz, NH_2CH_3). HRMS (ESI) calculated for $C_{22}H_{25}N_6O_2S$ $[M+H]^+$ 437.1754, found 437.1747.

4.2.7. 11-(3-Aminopropylamino)-4-(2-guanidinoethylamino) anthra[2,3-b]thiophene-5,10-dione dihydrochloride (**13**)

This compound was prepared from **8** and 1,3-diaminopropane as described for **11**. A dark blue powder, yield 68%, mp 201–203 °C. HPLC (LW = 266 nm, gradient B 10 → 60% (25 min)) t_R = 12.70 min, purity 95.8%. ^{1}H NMR (400 MHz, DMSO-d_6) δ 12.38 (br s, 1H, NH), 12.14 (br s, 1H, NH), 8.25 (m, 3H, 2-H, 6-H, 9-H), 8.09 (br s, 3H, NH_3), 8.02 (d, 1H, J = 5.5 Hz, 3-H), 7.88 (t, 1H, J = 5.6 Hz, NH), 7.77 (m, 2H, 7-H, 8-H), 7.33 (br s, 4H, $2NH_2$), 4.01 (m, 2H, $HNCH_2$), 3.91 (m, 2H, $HNCH_2$), 3.59 (m, 2H, $HNCH_2CH_2$), 3.31 (m, 2H, $HNCH_2$ CH_2CH_2), 2.07 (m, 2H, $HNCH_2$ CH_2CH_2). HRMS (ESI) calculated for $C_{22}H_{25}N_6O_2S$ $[M+H]^+$ 437.1754, found 437.1743.

4.2.8. 4-Amino-11-(2-guanidinoethylamino)anthra[2,3-b] thiophene-5,10-dione hydrochloride (**14**)

This compound was prepared from **9** as described for **10**. A dark violet powder, yield 78%, mp 258–260 °C. HPLC (LW = 264 nm, gradient B 30 → 70% (30 min)) t_R = 10.66 min, purity 97.1%. ^{1}H NMR (400 MHz, DMSO-d_6) δ 11.41 (t, 1H, J = 5.1 Hz, NH), 8.28 (m, 4H, 6-H, 9-H, NH_2), 8.23 (d, 1H, J = 5.6 Hz, 2-H), 8.18 (d, 1H, J = 5.6 Hz, 3-H), 7.79 (m, 2H, 7-H, 8-H), 7.74 (br s, 1H, NH), 7.20 (br s, 4H, $2NH_2$), 4.06 (m, 2H, $HNCH_2$), 3.56 (m, 2H, CH_2NH). HRMS (ESI) calculated for $C_{19}H_{18}N_5O_2S$ $[M+H]^+$ 380.1176, found 380.1170.

4.2.9. 4-(2-Guanidinoethylamino)-11-(2-(methylamino) ethylamino)anthra[2,3-b]thiophene-5,10-dione dihydrochloride (**15**)

This compound was prepared from **9** and N-methylethylenediamine as described for **11**. A dark blue powder, yield 72%, mp 199–201 °C. HPLC (LW = 266 nm, gradient B 10 → 60% (25 min)) t_R = 12.91 min, purity 98.0%. ^{1}H NMR (400 MHz, DMSO-d_6) δ 12.18 (br s, 1H, NH), 11.73 (br s, 1H, NH), 8.59 (br s, 2H, 2NH), 8.28 (m, 3H, 2-H, 6-H, 9-H), 7.99 (d, 1H, J = 5.5 Hz, 3-H), 7.81 (m, 2H, 7-H, 8-H), 7.78 (t, 1H, J = 5.6 Hz, NH), 7.28 (br s, 4H, $2NH_2$), 4.07 (m, 2H, $HNCH_2$), 3.99 (m, 2H, $HNCH_2$), 3.45 (m, 2H, $HNCH_2CH_2$), 3.33 (m, 2H, $HNCH_2CH_2$), 2.66 (s, 3H, NH_2CH_3). HRMS (ESI) calculated for $C_{22}H_{25}N_6O_2S$ $[M+H]^+$ 437.1754, found 437.1750.

4.3. FRET melting assay

The ability of anthrathiophenediones to stabilize TelQ formed by TelQ22-DA oligonucleotide in the presence of potassium ions, was studied by FRET melting assay [18]. Data were also used to evaluate compounds' affinities to TelQ. Experiments were performed on an ABI 7500 real-time PCR system (Applied Biosystems, Foster City, USA) in 96-well PCR plates (semi-skirt, raised rim, transparent) with standard ABI-type wells (thin-walled, 200 μl). Melting of samples was monitored by measuring FAM fluorescence intensity using the filter for FAM/SYBR Green. Fluorescence was recorded at 20–95 °C with a 0.5 °C increment. Constant temperature was maintained for 30 s prior to each measurement to ensure stable values. The reaction mixture (total volume 25 μl) contained 0.1 μM TelQ22-DA oligonucleotide in the buffer (10 mM Na phosphate pH 7.8, 80 mM LiCl, 10 mM KCl) in the absence or presence of the tested compound (1 μM). To assess the binding selectivity to TelQ *vs* duplex DNA, increasing concentrations of self-complementary ds26 oligonucleotide were added to 0.1 μM TelQ22-DA and 1 μM of the tested compound. Each well was triplicated, experiments were repeated 3 times. The melting temperature T_m was determined as the point of maximum in the first derivative of the melting curve.

4.4. G4-FID assay

This method is based on the change of fluorescence of the DNA light-up probe TO after its ligand-induced displacement from DNA quadruplexes [28]. Samples contained 0.25 μM TelQ24, 10 mM Na phosphate buffer pH 7.8, 100 mM KCl and 1 μM TO. Anthrathiophenedione derivatives were added up to 2.5 μM (final concentration). The assays were run at 25 °C. TO displacement was monitored by reduction of its fluorescence (λ_{ex} = 505 nm, λ_{em} = 530 nm) in 1 cm (200 μl) quartz cell on a spectrofluorimeter (Photon Technology International, Inc., Pemberton Township, USA).

4.5. Isothermal titration calorimetry

Thermodynamic parameters of anthrathiophendiones' binding to TelQ22 were measured using an iTC200 instrument (MicroCal, Northampton, USA) as described [4]. Experiments were carried out

at 25 °C in 10 mM sodium phosphate buffer pH 6.5, 100 mM KCl. Aliquots (1.3 μl) of anthrathiophendione solution were injected into a 200 μl calorimetric cell containing TelQ22 to achieve the complete binding isotherm. The concentrations of TelQ22 in the cell were 1.5–5 μM; the anthrathiophendione concentration in the syringe was 500 μM. The heat of dilution was measured by injecting the anthrathiophendione solution into the buffer. The obtained values were subtracted from the reaction heat to get the effective heat of binding. The resulting titration curves were fitted using 'one set of sites' model on MicroCal Origin software. The binding constant K_b, enthalpy changes ΔH and stoichiometry N were determined. The entropy variation (ΔS) was calculated according to the standard thermodynamic equation.

4.6. Modulation of telomerase activity by anthrathiophenedione derivatives

The HEK293T cells were transfected with 2 μg p-DS-SFFV-hTERT and 20 μg pBluescript-DS-U1-hTR plasmids [23,29]. Two days post transfection cells were plated onto a T150 flask, propagated for 48 h and lysed (30 min, 4 °C) in 10 mL of ice-cold buffer (10 mM Tris–HCl pH 7.5, 1 mM $MgCl_2$, 1 mM EDTA, 0.1 mM phenylmethylsulfonyl fluoride, 5 mM β-mercaptoethanol, 1 mM dithiotreitol, 0.5% 3-[(3-cholamidopropyl)dimethylammonio]-1-propane sulfonate; CHAPS) supplemented with 10% glycerol. The lysate was centrifuged at 16.000 g for 30 min at 4 °C. The supernatant (S16 lysate) was immediately purified (see below). Tubes for centrifugation of samples were blocked with 6 mg/mL bovine serum albumin for 2 h. Five mL of S16 lysate were layered on 1 mL of CHAPS containing 20% glycerol and centrifuged at 100,000 g for 45 min at 4 °C. The supernatant was layered on top of 1 mL CHAPS containing 20% glycerol and then centrifuged at 210,000 g for 2 h at 4 °C (Optima MAX-XP Ultracentrifugation, Beckman Coulter, Miami, USA). The pellet was dissolved in 1 mL of TRAP buffer (20 mM Tris–HCl pH 8.3, 63 mM KCl, 1.5 mM $MgCl_2$, 0.1 mg/mL BSA, 0.002% Tween-20, 1 mM EGTA) containing 10% glycerol, aliquoted, quickly frozen in liquid nitrogen and stored at −80 °C until experiments.

RQ-TRAP (Real-time Quantitative Telomeric Repeat Amplification Protocol) was performed in the two-tube manner [30,31] with minor modifications. To 5 μl of purified telomerase extract (diluted 1:25 with 1xTRAP buffer) 5 μl of tested compound (final concentrations 6.1 nM; 24 nM; 100 nM; 390 nM; 1.56 μM; 6.25 μM; 25 μM and 100 μM) in 1xTRAP buffer were added. The mixture was incubated for 10 min at room temperature, then 5 μl of the mixture containing 1xTRAP buffer, 0.3 μM oligonucleotide 5′-d(AATCCGTCGAGCAGAGTT)-3′ (telomerase substrate; TS, Lytech, Moscow, Russia) and 0.3 mM of each dNTP were added. After 30 min at 30 °C the mixture was heated (80 °C, 10 min) and diluted with 200 μl of 1xTRAP buffer. Then 5 μl of the diluted telomerase extract was further diluted with 200 μl of 1xTRAP buffer and used in PCR. The PCR reaction (total volume 10 μl) contained 5 μl of finally diluted telomerase extract, 1xTRAP buffer, 0.2 μM TS, 0.2 μM oligonucleotide 5′-d(GCGCGGCTTACCCTTACCCTTACCCTAACC)-3′ (ACX, Lytech, Moscow, Russia), 0.1 mM of each dNTP, 0.05 unit of Taq polymerase and 0.2× SYBR Green I (Invitrogen, Carlsbad, USA) [32]. Amplification was performed in a 384-well plate (CFX-384 Real-Time System, C1000 Thermal Cycler; Bio-Rad, Hercules, USA). Thirty PCR cycles consisted of 30 s at 95 °C, 30 s at 60 °C and 60 s at 72 °C. The experiments were repeated at least three times. The tested anthrathiophenedione derivatives were added prior to telomerase extension reaction or after the completion of this reaction (to estimate PCR inhibition), see Fig. 2. Determination of Ct value was performed automatically using a threshold line in Bio-Rad CFX Manager (version 1.6.541.1028). All calculations were performed in GraphPad Prism 5. In preliminary experiments we determined the concentrations of telomerase and its oligonucleotide substrate at which the increase of amplified DNA after telomerase extension was linear. To do so, the purified telomerase extract and the oligonucleotide containing the human telomeric repeat 5′-d(AATCCGTCGAGCAGAG(TTAGGG)$_7$-TTAG)-3′ (TSR8, Syntol, Moscow, Russia) were serially diluted followed by PCR amplification.

4.7. Topo I assay

The influence of compounds **1**, **2**, **11**, **13**–**15** on the activity of topo I was determined in a DNA relaxation assay [33]. Briefly, 1 unit of purified topo I (Promega, Fitchburg, USA) was incubated with 0.25 μg of supercoiled pBR322 plasmid DNA (Fermentas, Vilnius, Lithuania) in the buffer (35 mM Tris–HCl pH 8.0, 72 mM KCl, 5 mM $MgCl_2$, 5 mM dithiotreitol, 0.1% bovine serum albumin, 2 mM spermidine, 5% glycerol) in the presence of 0.1% DMSO (vehicle control) or tested compounds (final concentrations are indicated in Fig. 3) for 30 min at 37 °C. The reaction was terminated by the addition of 1% sarcosyl. Then proteinase K was added, and the reaction mixture was further incubated at 37 °C for 40 min. DNA topoisomers were resolved by electrophoresis in a 1% agarose gel (3 h, 70 V) in the buffer (40 mM Tris acetate pH 7.8, 1 mM EDTA, 30 mM acetic acid) and stained with ethidium bromide.

4.8. Cell culture, intracellular accumulation and growth inhibition assays

The murine leukemia L1210 and human CD4+ T-lymphocyte CEM cell line (American Type Culture Collection; Manassas, USA) were propagated in RPMI-1640 medium supplemented with 10% fetal calf serum, 0.075% $NaHCO_3$ and 2 mM L-glutamine, 100 units/mL penicillin, and 100 μg/mL streptomycin at 37 °C, 5% CO_2 in humidified atmosphere. Cells in logarithmic phase of growth were used in the experiments. New compounds were dissolved in 10% aqueous DMSO as 10 mM stock solutions followed by serial dilutions in water immediately before experiments.

For measurements of intracellular accumulation of anthrathiophenedione derivatives L1210 cells were plated into 35 mm Petri dishes (2×10^5 cells in 3 mL of culture medium) and treated with compounds **1**, **2** and **13** (1 μM each) for 15–360 min at 37 °C, 5% CO_2. After the completion of exposure cells were washed twice with cold saline and placed on ice. Cell associated fluorescence was immediately analyzed on a FACSCanto II (Becton Dickinson, San Jose, USA) at the excitation wavelength 633 nm and emission detected in the 660/20 nm channel. Fluorescence of untreated cells was used as a blank. Ten thousand events were collected per each sample. The channels corresponding to the peaks of Gaussian fluorescence distribution histograms were normalized to autofluorescence of solutions containing 1 μM of **1**, **2** or **13** in DMSO.

Cell proliferation assays were performed in 96-well microtiter plates. Each well contained (5–7.5) $\times$ 10^4 tumor cells and the increasing concentrations the tested compound. Cells were incubated for 48 h (L1210) or 72 h (CEM) at 37 °C in a humidified CO_2-controlled atmosphere, stained with trypan blue and counted in a Coulter counter. The IC_{50} was defined as the concentration of the compound that inhibited cell proliferation by 50%.

Acknowledgments

The authors are grateful to J. Lingner for plasmids, M. Vagida for assistance in flow cytometry, A. Korolev and N. Maliutina for HRMS and HPLS analyses, and L. van Berckelaer (KU Leuven) for help in cell proliferation assays. The study was supported by Molecular and

Cellular Biology Program of the Russian Academy of Sciences and by KU Leuven (GOA 10/014).

Appendix A. Supplementary data

Supplementary data related to this article can be found at http://dx.doi.org/10.1016/j.ejmech.2014.08.030.

References

[1] K. Krohn, Anthracycline Chemistry and Biology I: Biological Occurrence and Biosynthesis, Synthesis and Chemistry, Springer, 2008, http://dx.doi.org/10.1007/978-3-540-75815-0.

[2] L.H. Hurley, DNA and its associated processes as targets for cancer therapy, Nat. Rev. Cancer 2 (2002) 188–200, http://dx.doi.org/10.1038/nrc749.

[3] D. Sun, B. Thompson, B.E. Cathers, M. Salazar, S.M. Kerwin, J.O. Trent, T.C. Jenkins, S. Neidle, L.H. Hurley, Inhibition of human telomerase by a G-quadruplex-interactive compound, J. Med. Chem. 40 (1997) 2113–2116, http://dx.doi.org/10.1021/jm970199z.

[4] D. Kaluzhny, N. Ilyinsky, A. Shchekotikhin, Y. Sinkevich, P.O. Tsvetkov, V. Tsvetkov, A. Veselovsky, M. Livshits, O. Borisova, A. Shtil, A. Shchyolkina, Disordering of human telomeric G-quadruplex with novel antiproliferative anthrathiophenedione, PLoS One 6 (2011) e27151, http://dx.doi.org/10.1371/journal.pone.0027151.

[5] A.E. Shchekotikhin, V.A. Glazunova, L.G. Dezhenkova, Y.N. Luzikov, Y.B. Sinkevich, L.V. Kovalenko, V.N. Buyanov, J. Balzarini, F.C. Huang, J.J. Lin, H.S. Huang, A.A. Shtil, M.N. Preobrazhenskaya, Synthesis and cytotoxic properties of 4,11-bis[(aminoethyl)amino]anthra[2,3-b]thiophene-5,10-diones, novel analogues of antitumor anthracene-9,10-diones, Bioorg. Med. Chem. 17 (2009) 1861–1869, http://dx.doi.org/10.1016/j.bmc.2009.01.047.

[6] S. Cogoi, A.E. Shchekotikhin, A. Membrino, Y.B. Sinkevich, L.E. Xodo, Guanidino anthrathiophenediones as G-quadruplex binders: uptake, intracellular localization, and anti-harvey-ras gene activity in bladder cancer cells, J. Med. Chem. 56 (2013) 2764–2778, http://dx.doi.org/10.1021/jm3019063.

[7] A.S. Reddy, S. Zhang, Polypharmacology: drug discovery for the future, Expert Rev. Clin. Pharmacol. 6 (2013) 41–47, http://dx.doi.org/10.1586/ecp.12.74.

[8] A.D. Boran, R. Iyengar, Systems approaches to polypharmacology and drug discovery, Curr. Opin. Drug Discov. Dev. 13 (2010) 297. http://www.ncbi.nlm.nih.gov/pmc/articles/PMC3068535/.

[9] A.L. Hopkins, Network pharmacology: the next paradigm in drug discovery, Nat. Chem. Biol. 4 (2008) 682–690, http://dx.doi.org/10.1038/nchembio.118.

[10] B. Clement, Reduction of N-hydroxylated compounds: amidoximes (N-hydroxyamidines) as pro-drugs of amidines, Drug Metab. Rev. 34 (2002) 565–579, http://dx.doi.org/10.1081/DMR-120005643.

[11] J. Sun, A. Dahan, G.L. Amidon, Enhancing the intestinal absorption of molecules containing the polar guanidino functionality: a double-targeted prodrug approach, J. Med. Chem. 53 (2009) 624–632, http://dx.doi.org/10.1021/jm9011559.

[12] Y.B. Sinkevich, A.E. Shchekotikhin, Y.N. Luzikov, V.N. Buyanov, L.V. Kovalenko, Synthesis of thiopheno-quinizarine derivatives, Chem. Heterocycl. Compd. 43 (2007) 1252–1259, http://dx.doi.org/10.1007/s10593-007-0191-x.

[13] S. Neidle, Human telomeric G-quadruplex: the current status of telomeric G-quadruplexes as therapeutic targets in human cancer, FEBS J. 277 (2010) 1118–1125, http://dx.doi.org/10.1111/j.1742-4658.2009.07463.x.

[14] G.W. Collie, G.N. Parkinson, The application of DNA and RNA G-quadruplexes to therapeutic medicines, Chem. Soc. Rev. 40 (2011) 5867–5892, http://dx.doi.org/10.1039/c1cs15067g.

[15] C. Sissi, B. Gatto, M. Palumbo, The evolving world of protein-G-quadruplex recognition: a medicinal chemist's perspective, Biochimie 93 (2011) 1219–1230, http://dx.doi.org/10.1016/j.biochi.2011.04.018.

[16] S. Balasubramanian, L.H. Hurley, S. Neidle, Targeting G-quadruplexes in gene promoters: a novel anticancer strategy? Nat. Rev. Drug Discov. 10 (2011) 261–275, http://dx.doi.org/10.1038/nrd3428.

[17] J.L. Mergny, L. Lacroix, Analysis of thermal melting curves, Oligonucleotides 13 (2003) 515–537, http://dx.doi.org/10.1089/154545703322860825.

[18] A. De Cian, L. Guittat, M. Kaiser, B. Sacca, S. Amrane, A. Bourdoncle, P. Alberti, M.P. Teulade-Fichou, L. Lacroix, J.L. Mergny, Fluorescence-based melting assays for studying quadruplex ligands, Methods 42 (2007) 183–195, http://dx.doi.org/10.1016/j.ymeth.2006.10.004.

[19] D. Monchaud, C. Allain, H. Bertrand, N. Smargiasso, F. Rosu, V. Gabelica, A. De Cian, J.-L. Mergny, M.-P. Teulade-Fichou, Ligands playing musical chairs with G-quadruplex DNA: a rapid and simple displacement assay for identifying selective G-quadruplex binders, Biochimie 90 (2008) 1207–1223, http://dx.doi.org/10.1016/j.biochi.2008.02.019.

[20] N.W. Kim, F. Wu, Advances in quantification and characterization of telomerase activity by the telomeric repeat amplification protocol (TRAP), Nucleic Acids Res. 25 (1997) 2595–2597, http://dx.doi.org/10.1093/nar/25.13.2595.

[21] M. Hou, D. Xu, M. Bjorkholm, A. Gruber, Real-time quantitative telomeric repeat amplification protocol assay for the detection of telomerase activity, Clin. Chem. 47 (2001) 519–524. http://www.clinchem.org/content/47/3/519.full.

[22] H. Wege, M.S. Chui, H.T. Le, J.M. Tran, M.A. Zern, SYBR green real-time telomeric repeat amplification protocol for the rapid quantification of telomerase activity, Nucleic Acids Res. 31 (2002), http://dx.doi.org/10.1093/nar/gng003 e3–e3.

[23] E.P. Cohn, K.-L. Wu, T.R. Pettus, N.O. Reich, A new strategy for detection and development of tractable telomerase inhibitors, J. Med. Chem. 55 (2012) 3678–3686, http://dx.doi.org/10.1021/jm201191d.

[24] D. D'Ambrosio, P. Reichenbach, E. Micheli, A. Alvino, M. Franceschin, M. Savino, J. Lingner, Specific binding of telomeric G-quadruplexes by hydrosoluble perylene derivatives inhibits repeat addition processivity of human telomerase, Biochimie 94 (2012) 854–863, http://dx.doi.org/10.1016/j.biochi.2011.12.004.

[25] G. Schwarzenbach, K. Lutz, Aciditätsmessungen an mesomeren Säuren und Basen. Einige Aussagen über die Resonanzenergie, Helv. Chim. Acta 23 (1940) 1162–1190, http://dx.doi.org/10.1002/hlca.194002301141.

[26] L. Fabbrizzi, M. Micheloni, P. Paoletti, G. Schwarzenbach, Protonation processes of unusual exothermicity, J. Am. Chem. Soc. 99 (1977) 5574–5576, http://dx.doi.org/10.1021/ja00459a006.

[27] P.J. Perry, A.P. Reszka, A.A. Wood, M.A. Read, S.M. Gowan, H.S. Dosanjh, J.O. Trent, T.C. Jenkins, L.R. Kelland, S. Neidle, Human telomerase inhibition by regioisomeric disubstituted amidoanthracene-9, 10-diones, J. Med. Chem. 41 (1998) 4873–4884, http://dx.doi.org/10.1021/jm981067o.

[28] D. Monchaud, M.P. Teulade-Fichou, G4-FID: a fluorescent DNA probe displacement assay for rapid evaluation of quadruplex ligands, Methods Mol. Biol. 608 (2010) 257–271, http://dx.doi.org/10.1007/978-1-59745-363-9_15.

[29] D.V. Vasilkova, D.M. Azhibek, T.S. Zatsepin, Y.V. Naraikina, V.S. Prassolov, M.M. Prokofjeva, M.I. Zvereva, M.P. Rubtsova, Dynamics of human telomerase RNA structure revealed by antisense oligonucleotide technique, Biochimie 95 (2013) 2423–2428, http://dx.doi.org/10.1016/j.biochi.2013.09.001.

[30] B. Fu, J. Quintero, C.C. Baker, Keratinocyte growth conditions modulate telomerase expression, senescence, and immortalization by human papillomavirus type 16 E6 and E7 oncogenes, Cancer Res. 63 (2003) 7815–7824 cancerres.aacrjournals.org/content/63/22/7815.long.

[31] K.S. Hathcock, R.J. Hodes, N.-P. Weng, Analysis of telomere length and telomerase activity, in: R. Coico (Ed.), Current Protocols in Immunology, John Wiley & Sons, Inc., 2004, pp. 10.30.11–10.30.27, http://dx.doi.org/10.1002/0471142735.im1030s62.

[32] S. Prevost, N. Arbour, C. Harder, SYBR® Green I Concentrations for Real-time PCR, 2007. http://www.researchgate.net/publication/239558185_SYBR_Green_I_concentrations_for_real-time_PCR.

[33] A.E. Shchekotikhin, V.A. Glazunova, L.G. Dezhenkova, E.K. Shevtsova, V.F. Traven, J. Balzarini, H.-S. Huang, A.A. Shtil, M.N. Preobrazhenskaya, The first series of 4, 11-bis [(2-aminoethyl) amino] anthra [2, 3-*b*] furan-5, 10-diones: synthesis and anti-proliferative characteristics, Eur. J. Med. Chem. 46 (2011) 423–428, http://dx.doi.org/10.1016/j.ejmech.2010.11.017.